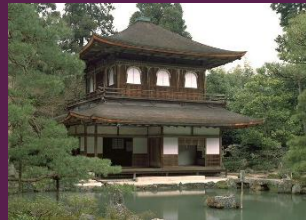


# Eikonal method for halo nuclei

E. C. Pinilla, P. Descouvemont and D. Baye

Université Libre de Bruxelles, Brussels, Belgium



**YIPQS Long-term workshop**

**Dynamics and Correlations in Exotic Nuclei (DCEN2011)**

20th September - 28th October, 2011

Yukawa Institute for Theoretical Physics, Kyoto, Japan

# Outline

## 1. Motivation

## 2. Introduction

## 3. Four-body eikonal method

- Elastic scattering  ${}^9\text{Li}+n+n$  on  ${}^{208}\text{Pb}$  @ 70 A MeV
- Breakup of  ${}^9\text{Li}+n+n$  on  ${}^{208}\text{Pb}$  @ 70 A MeV

## 4. Three-body projectile

- Bound states
- Scattering states

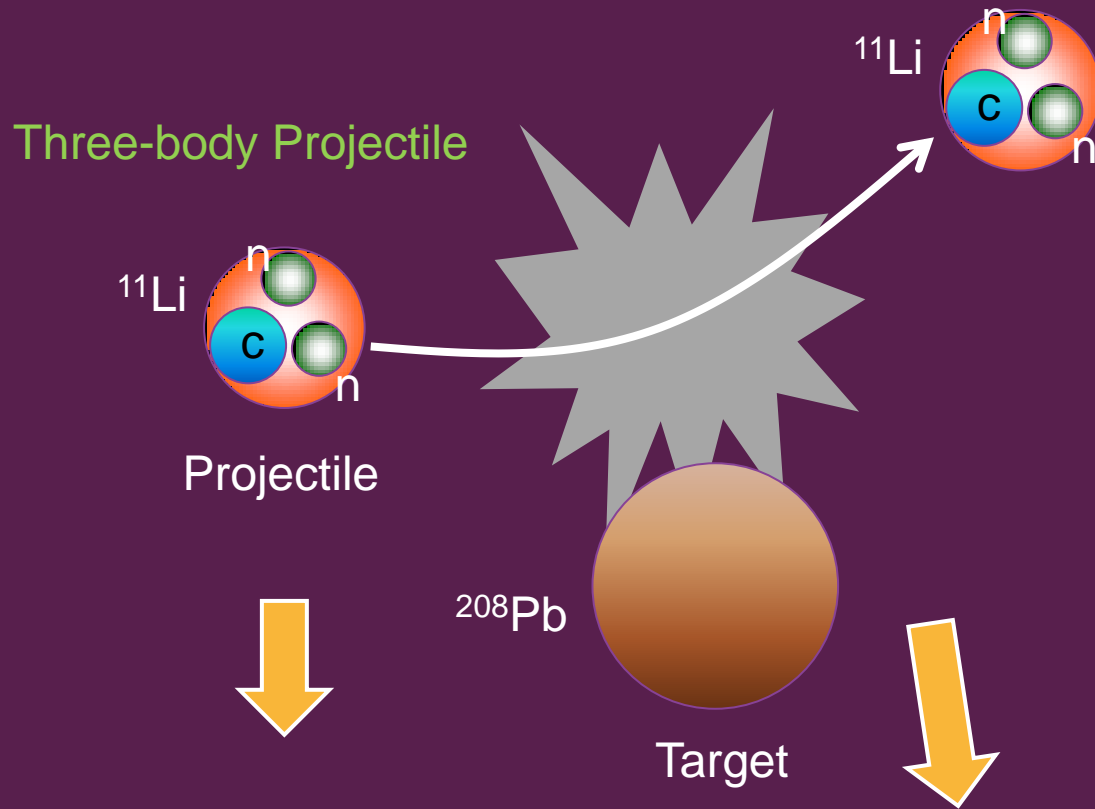
## 5. Applications

- ${}^6\text{He}$
- Nucleus of our interest  ${}^{11}\text{Li}$

## 6. Conclusions

# Motivation

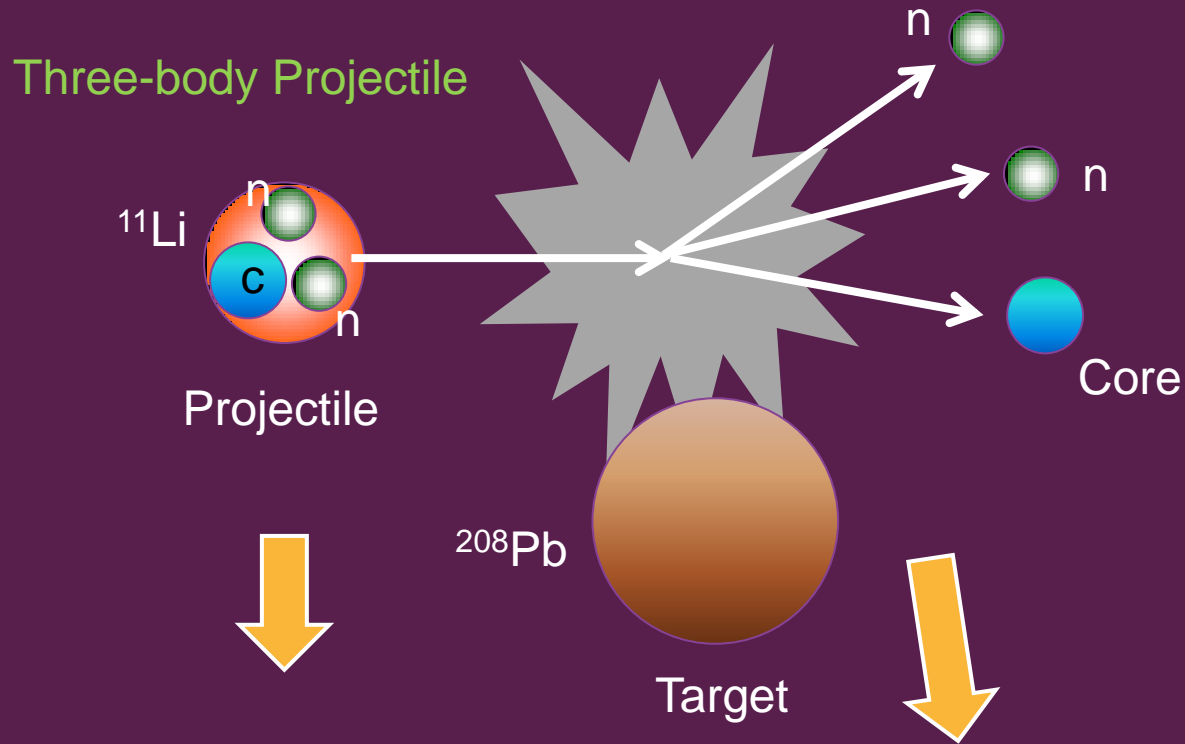
To study elastic scattering and breakup cross sections of  $^{11}\text{Li}$  in a four-body eikonal model.



- Bound states
- Continuum states
- Dipole strengths
- Four-body elastic scattering cross sections

# Motivation

To study elastic scattering and breakup cross sections of  $^{11}\text{Li}$  in a four-body eikonal model.

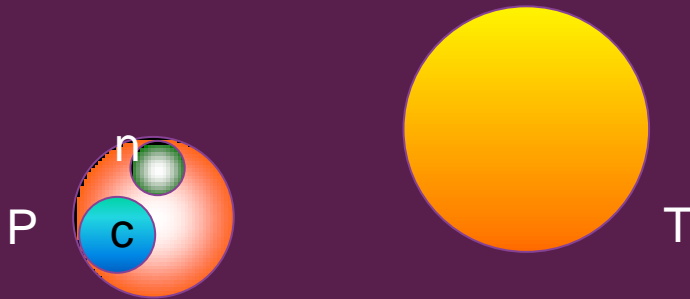


- Bound states
- Continuum states
- Dipole strengths
- Breakup cross sections
- Angular distributions

# Introduction

- ❖ **High-energy reactions** are widely used to investigate Halo nuclei.
- ❖ High incident energies permits to handle the Schrödinger equation in a simplified way: **Eikonal approximation**.
- ❖ Non-microscopic 2-Body and 3-Body descriptions of the projectile has been introduced in the eikonal method.

Two-body projectile

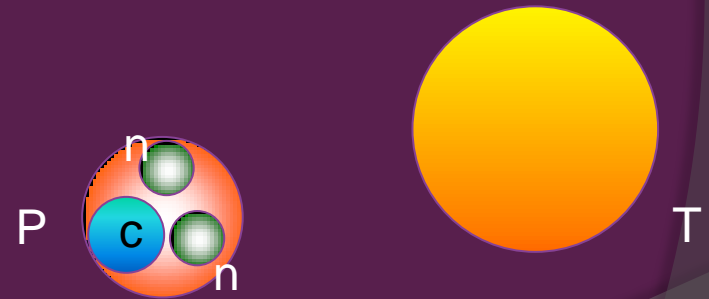


Elastic scattering, breakup

Ex:  $^{11}\text{Be} + ^{208}\text{Pb} = (^{10}\text{Be} + n) + ^{208}\text{Pb}$

G. Goldstein, et. al; Phys. Rev. C 73, 024602 (2006).

Three-body projectile



Elastic scattering, breakup

Ex:  $^6\text{He} + ^{208}\text{Pb} = (\alpha + n + n) + ^{208}\text{Pb}$

D. Baye, et. al; Phys. Rev. C 79, 024607 (2009).

# Eikonal approximation for one-body projectile

We have to solve the Schrödinger equation

$$\left[ -\frac{\hbar^2}{2\mu_{PT}} \Delta + V_{PT}(r) \right] \Phi(\mathbf{r}) = E\Phi(\mathbf{r}).$$

At high-energies the wave function: **Smooth deviation from a plane wave**

$$\Phi(\mathbf{r}) = \frac{1}{(2\pi)^{3/2}} e^{iKZ} \hat{\Phi}(\mathbf{r}),$$

Smooth varying function

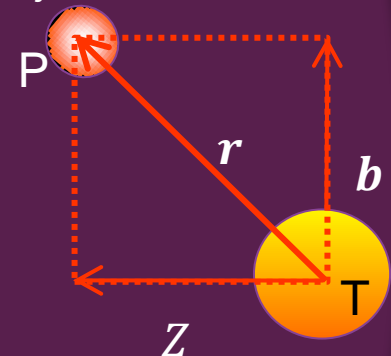
we have

$$-\frac{\hbar^2}{2\mu_{PT}} \left[ \Delta + 2iK \frac{\partial}{\partial Z} + V_{PT}(r) \right] \hat{\Phi}(\mathbf{r}) = 0.$$

At high-energies  $|\Delta \hat{\Phi}| \ll K \left| \frac{\partial \hat{\Phi}}{\partial Z} \right|$ , then

$$\Phi^{\text{eik}} = \frac{1}{(2\pi)^{3/2}} \exp\left[ iKZ - \frac{i}{\hbar v} \int_{-\infty}^Z V_{PT}(\mathbf{b}, Z') dZ' \right].$$

Structureless projectile



Structureless Target

# Eikonal approximation for one body projectile

Ex: Elastic scattering of an incident uncharged particle

The elastic amplitude

$$f(\theta) = iK \int_0^{\infty} J_0(qb) [1 - e^{i\chi(b)}] b db; \quad q = 2K \sin \frac{\theta}{2}$$

The eikonal phase

$$\chi(b) = -\frac{1}{\hbar v} \int_{-\infty}^{\infty} V_{PT}(b, Z) dZ; \quad v = \frac{\hbar K}{\mu_{PT}}$$

Extension to charge particles

$$\chi(b) = \underbrace{\chi_N(b)}_{\text{Nuclear}} + \underbrace{\chi_C(b)}_{\text{Coulomb}}$$

Corrected to overcome divergences due to the Coulomb potential.

# Elastic cross sections for $n+^{208}\text{Pb}$ at different incident energies

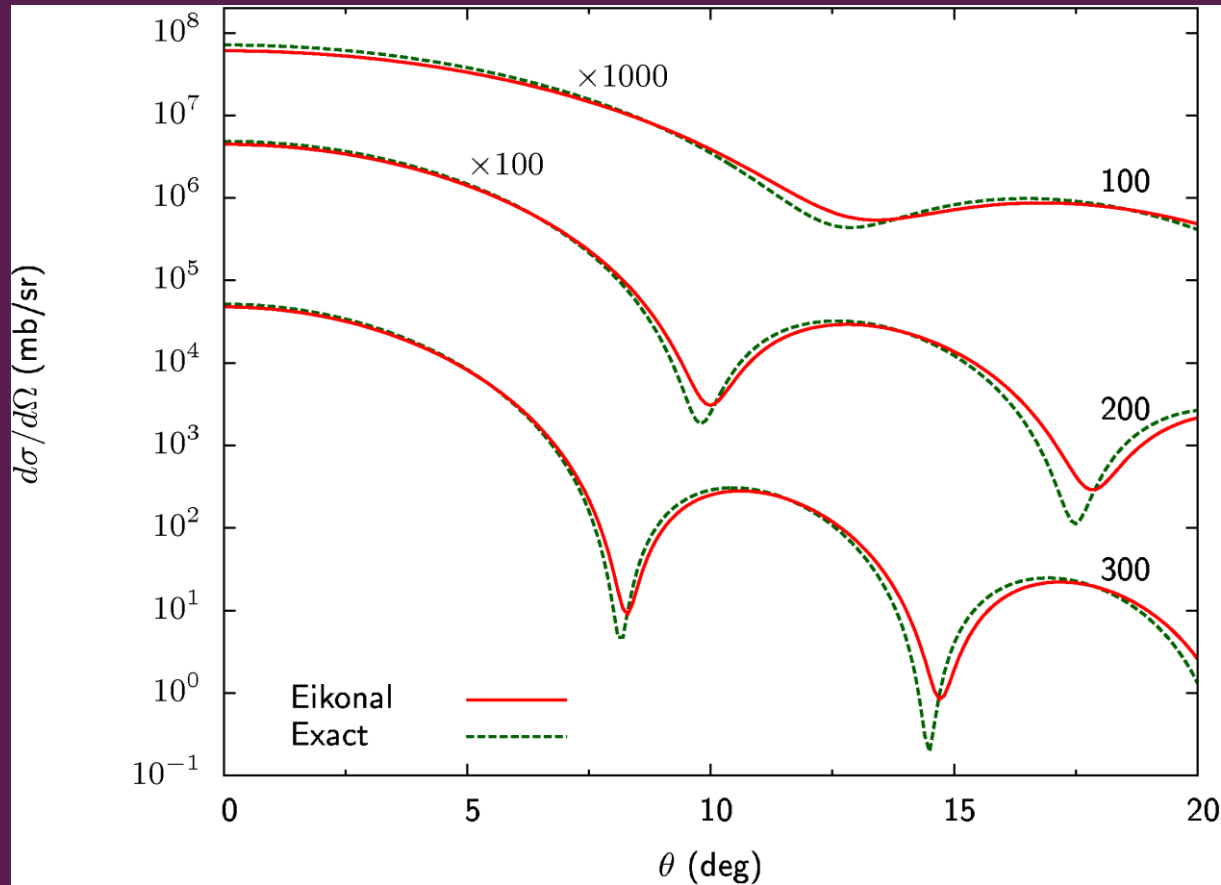
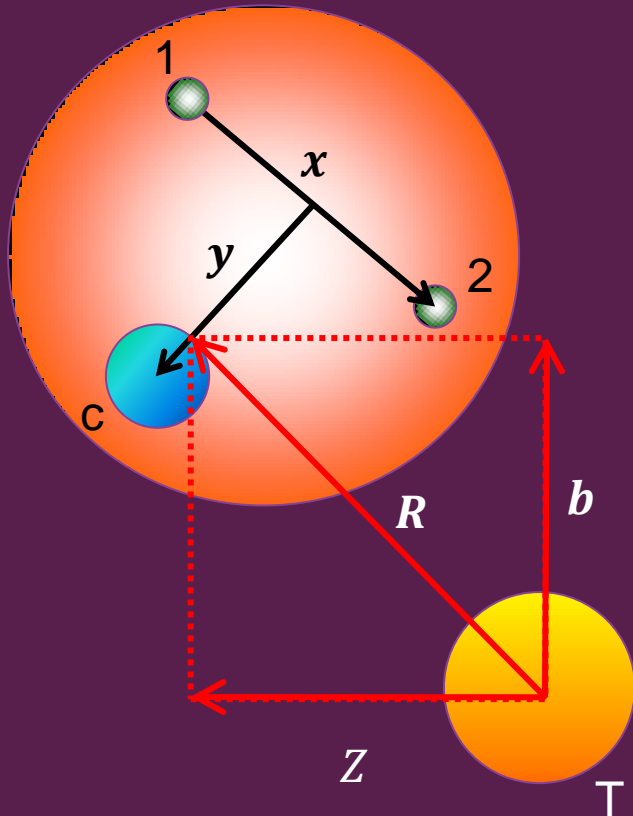


Fig 1. The energies are shown in MeV. The  $n+^{208}\text{Pb}$  potential is taken from A. J. Kooning and J. P. Delaroche, *Nucl. Phys. A* 713, 231 (2003).

❖ The agreement improves when the energy increases and  $\theta$  decreases.



# Four-body eikonal



$$H_{4B}\Phi = E_T\Phi, \quad E_T = E_0 + \frac{\hbar^2 K^2}{2\mu_{PT}}$$

$E_0 \rightarrow$  G. S. energy of the projectile

$\frac{\hbar^2 K^2}{2\mu_{PT}} \rightarrow$  Initial relative P.T. energy

$$H_{4B} = -\frac{\hbar^2}{2\mu_{PT}} \nabla_R^2 + V_{PT} + H_{3B},$$

Nuclear optical potentials+Coulomb

$$V_{PT} = V_{CT} + V_{Tn} + V_{Tn}$$

Factorizing:  $\Phi(\vec{R}, \vec{x}, \vec{y}) = e^{iKZ} \hat{\phi}(\vec{R}, \vec{x}, \vec{y})$

$$\rightarrow \left( -\frac{\hbar^2}{2\mu_{PT}} \nabla_R^2 - i\hbar\partial_Z + V_{PT} \right) \hat{\phi} = 0$$

The eikonal approx.  $|\nabla^2 \hat{\phi}| \ll K |\partial_Z \hat{\phi}|$   
(High-energies)

# Four-body eikonal

Eikonal w. f.  $\longrightarrow \hat{\Phi}^{\text{eik}}(\mathbf{R}, \mathbf{x}, \mathbf{y}) \approx \Psi_0(\mathbf{x}, \mathbf{y}) \exp \left[ -\frac{i}{\hbar v} \int_{-\infty}^Z V_{PT}(\mathbf{b}, \mathbf{Z}', \mathbf{x}, \mathbf{y}) dZ' \right]$

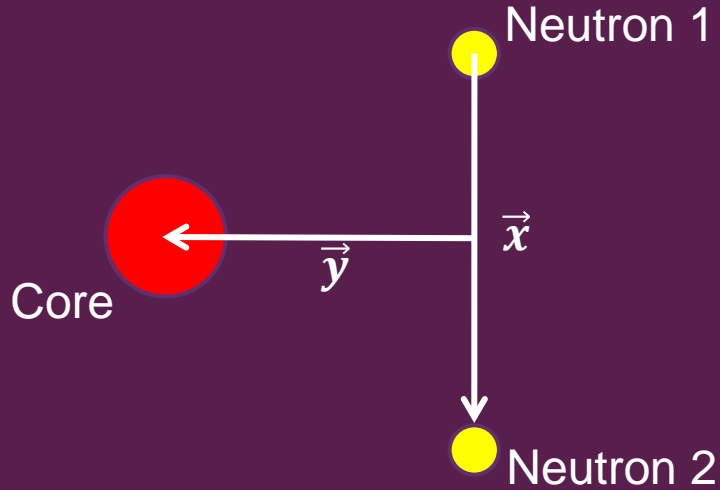
Eikonal elastic amplitude  $\longrightarrow S(\mathbf{b}) = \underbrace{\langle \Psi_{J_0 M_0' \pi_0} |}_{\text{3B bound state}} e^{i\chi(\mathbf{b})} \underbrace{ | \Psi_{J_0 M_0 \pi_0} \rangle}_{\text{3B bound state}} \longrightarrow \text{Elastic Cross sections}$

Eikonal breakup amplitude  $\longrightarrow S(\mathbf{b}) \propto \underbrace{\langle \Psi_{k_x K_y}(E) |}_{\text{3B scattering State R-matrix}} e^{i\chi(\mathbf{b})} \underbrace{ | \Psi_{J_0 M_0 \pi_0} \rangle}_{\text{3B bound state}} \longrightarrow \text{Bup obs.}$

$\swarrow$   
1-, 0+, 2+

Eikonal phase (Dynamics information)  $\longrightarrow \chi(\mathbf{b}) = -\frac{i}{\hbar v} \int_{-\infty}^{\infty} [V_{CT}(\mathbf{b}) + V_{nT}(\mathbf{b}) + V_{nT}(\mathbf{b})] dZ$

# Three-body model of the projectile



$\vec{x}, \vec{y}$ : Jacobi coordinates

$\rho, \alpha$ : Hyperspherical coordinates

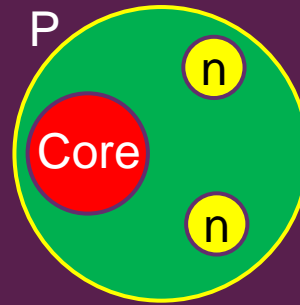
$\rho^2 = x^2 + y^2$ : Hyperradius

$\alpha = \arctan\left(\frac{y}{x}\right)$ : Hyperangle

$\Omega_5 = (\alpha, \Omega_x, \Omega_y)$

$$H_{3B}\Psi^{J\pi} = E\Psi^{J\pi}$$

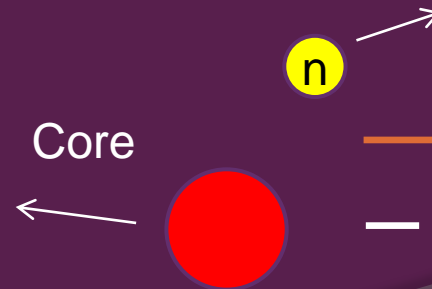
$E < 0 \rightarrow$  Bound state



----- 0 MeV, core + n + n

—————  $E_0 = -S_{2n}$

$E > 0 \rightarrow$  Scattering states



—————  $E$

----- 0 MeV, core + n + n

# Three-body model of the projectile

$$H_{3B} \Psi^{J\pi} = E \Psi^{J\pi}$$

$$H_{3B} = -\frac{\hbar^2}{2m_n} \nabla_x^2 - \frac{\hbar^2}{2m_n} \nabla_y^2 + T_{c.m.} + \sum_{i < j} V_{ij}$$

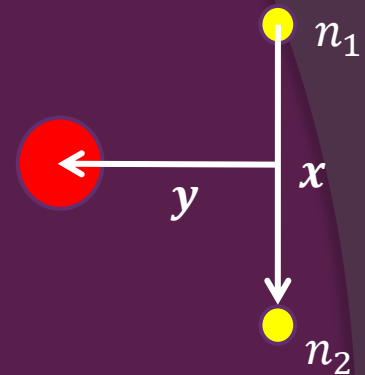
2B potentials, Vcn Gaussian, W. Saxon

$$\Psi^{J\pi} = \rho^{-5/2} \sum_{K=0}^{\infty} \sum_{\gamma} \chi_{\gamma K}^{J\pi}(\rho) \mathcal{Y}_{\gamma K}^{JM}(\Omega_5)$$

Hyperradial Function  
(Unknown)

Eigenfunction of angular  
momentum  $K$  (Known)

$\pi = (-1)^K \rightarrow$  Parity of the relative motion of the 3B



Spinless core

$$\gamma = (l_x, l_y, L, S)$$

$$\hat{L} = \hat{l}_x + \hat{l}_y$$

$$\hat{S} = \hat{S}_1 + \hat{S}_2$$

$$\hat{J} = \hat{L} + \hat{S}$$

# Three-body bound states

$$H_{3B}\Psi^{J\pi} = E\Psi^{J\pi}$$

$$\Psi^{J\pi} = \rho^{-5/2} \sum_{K=0}^{\infty} \sum_{\gamma} \chi_{\gamma K}^{J\pi}(\rho) \mathcal{Y}_{\gamma K}^{JM}(\Omega_5)$$

$$\chi_{\gamma K}^{J\pi}(\rho) = \sum_{i=1}^N c_{\gamma Ki}^{J\pi} u_i(\rho),$$

Eigenvalue problem

Lagrange basis

It facilitates the calculations

# Three-body continuum states: R-matrix

Internal region

$$\chi_{\gamma K}^{J\pi}(\rho) = \sum_{i=1}^N C_{\gamma Ki}^{J\pi} u_i(\rho)$$

External region

$$\chi_{\gamma K}^{J\pi}(\rho \rightarrow \infty)$$

$a$

$\rho$

Nuclear + Coulomb + Centrifugal potentials

Coulomb + Centrifugal potentials

$$\chi_{\gamma K}^{J\pi}(\rho \rightarrow \infty) = A_{\gamma K}^{J\pi} \left[ H_{\gamma K}^{-}(k\rho) \delta_{\gamma\gamma'} \delta_{KK'} - U_{\gamma K, \gamma' K'}^{J\pi} H_{\gamma K}^{+}(k\rho) \right]$$

Hankel functions

$U_{\gamma K, \gamma' K'}^{J\pi} \rightarrow$  Collision matrix  $\rightarrow e^{2i\delta} \rightarrow$  Eigenphases

Large matrix for typical  $\gamma K$  values

# Dimension of the R-matrix calculations

J=0 <sup>+</sup>		J=1 <sup>-</sup>		J=2 <sup>+</sup>	
Kmax	$\gamma K$	Kmax	$\gamma K$	Kmax	$\gamma K$
12	28	9	40	12	99
16	45	13	77	16	172
20	66	17	126	20	265

$$\gamma = (l_x, l_y, L, S)$$

$N \rightarrow$  Number of Lagrange basis, typical  $N = 40$

$\gamma K \rightarrow$  Channels number

Matrices of  $\rightarrow \gamma K N \times \gamma K N$

Example:  $J = 2^+$  and  $K_{\max} = 20$

Matrices of  $\rightarrow \gamma K N \times \gamma K N = 265 \cdot 40 \times 265 \cdot 40 = 10600 \times 10600$

# Applications for ${}^6\text{He}$ : Three-body resonances

- ❖  $R^{J\pi} \longrightarrow U^{J\pi} \longrightarrow (S^{-1}US = e^{2i\delta})$
- ❖ Information about three-body resonances is contained in the eigenphases  $\delta$ .

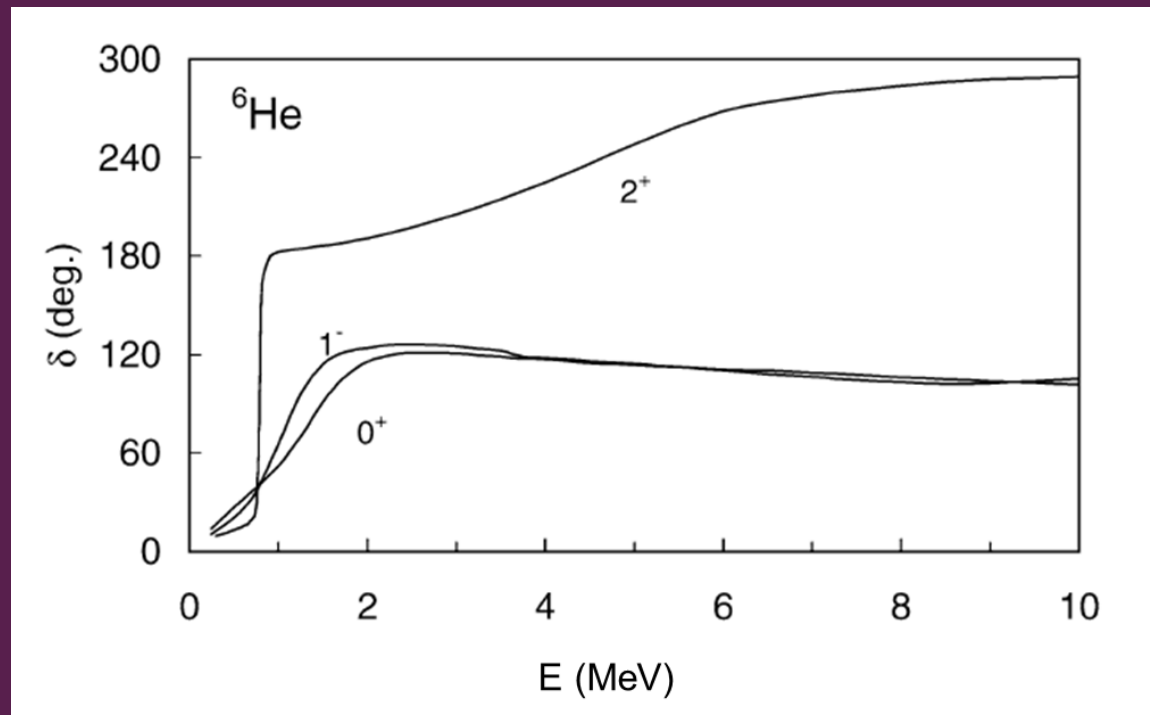


Fig. 2. Eigenphases for  ${}^6\text{He}$  for different  $J$  values (From *P. Descouvemont et al, Nucl. Phys. A 765 (2006) 370*).



# Applications for ${}^6\text{He}$ : E1 strength distribution

$$\frac{dB_{E1}}{dE}(E) \propto \left| \underbrace{\langle \Psi_{k_x k_y}(E) |}_{1^- \text{ 3B cont. R-matrix}} \mathcal{M}^{E1} \underbrace{|\Psi_{J_0 M_0 \pi_0}\rangle}_{0^+ \text{ 3B bound state}} \right|^2$$

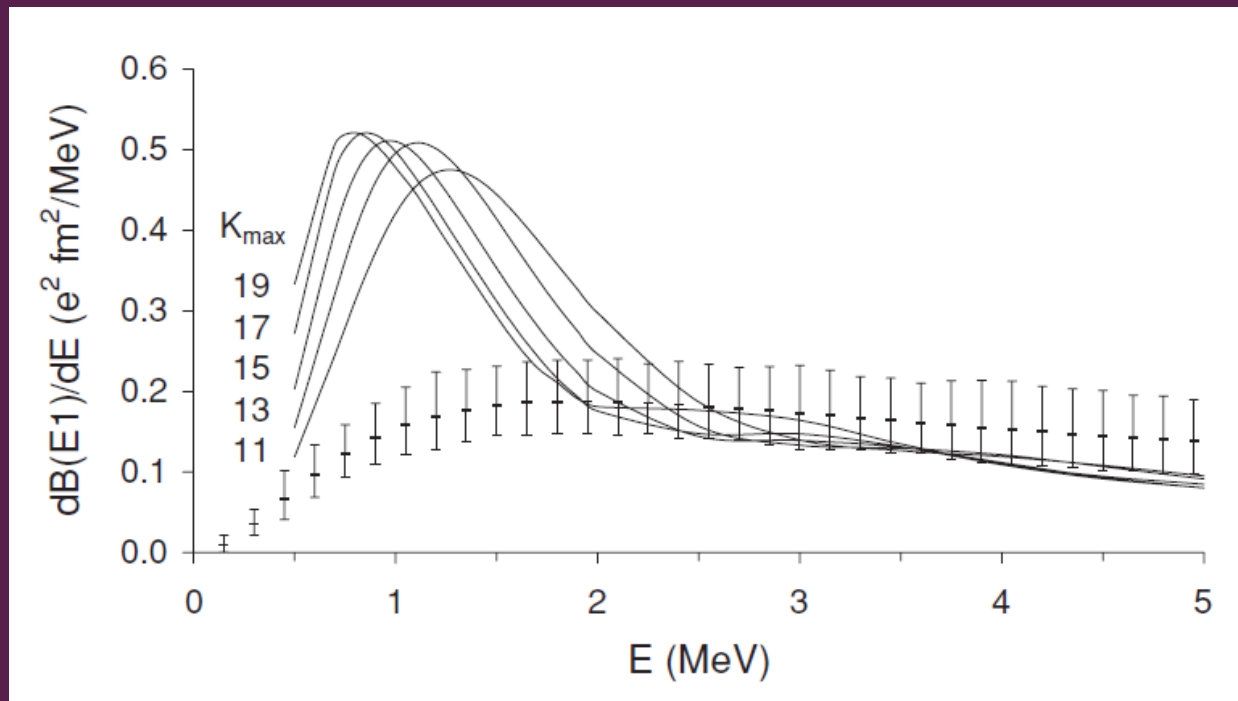


Fig. 3. Electric dipole distribution for different  $K_{\text{max}}$  values. From *D. Baye et al, Phys. Rev. C 79, 024607 (2009)*.

# Applications in $^{11}\text{Li}$ : Conditions of the calculations

To calculate bound and scattering states of  $^9\text{Li}+n+n$

## $^9\text{Li}+n$ interaction

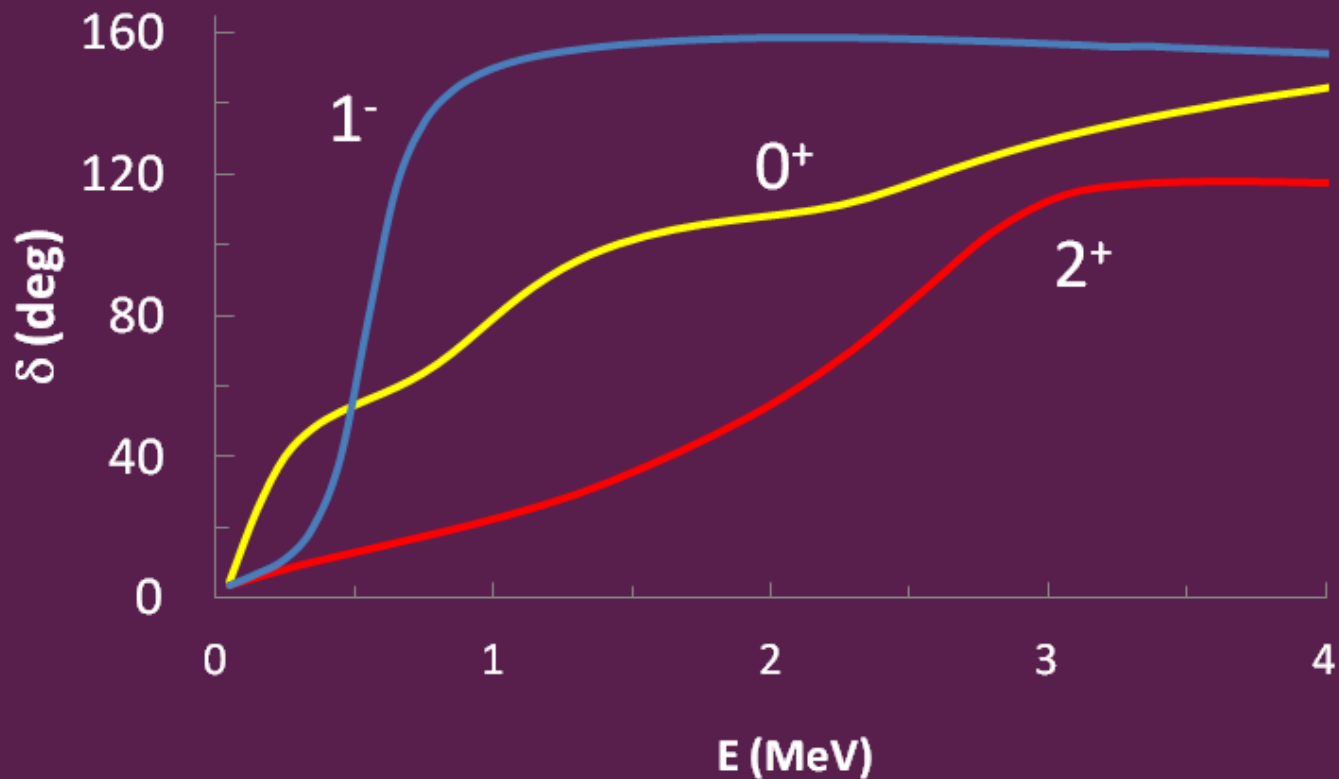
- ❖ From *H. Esbensen, et. al, Phys. Rev. C 56, 3054 (97)*.
- ❖ Non-existent elastic scattering experimental data.
- ❖ Fitted to reproduce a presumed  $p_{1/2}$  resonance at 540 keV and a  $s$  virtual state.
- ❖  $^9\text{Li}-n$  interaction multiplied by 1.0056 to reproduce **G.S. energy of  $^{11}\text{Li} = -0.378 \text{ MeV}$ .**

## $n+n$ potential

- ❖ Minnesota interaction

We those potentials we well reproduce **r.m.s. radius of  $^{11}\text{Li} : 3.1 \text{ fm}$  (exp. r.m.s. of  $3.16 \pm 0.11 \text{ fm}$ ).**

# Eigenphases of $^{11}\text{Li}$ in a three-body model



- ❖ Like-resonant behavior for  $1^-$  and  $2^+$  continuum
- ❖ Rise of the  $0^+$  phase shift with energy: “Like a superposition of resonances”

# Convolved E1 strength distribution of $^{11}\text{Li}$ with the detector response

R-matrix (Red curve)

$$\frac{dB_{E1}}{dE}(E) \propto \underbrace{\left| \Psi_{k_x k_y}(E) \right|}_{1^-} \underbrace{\left| \mathcal{M}^{E1} \Psi_{J_0 M_0 \pi_0} \right|}_{0^+}^2$$

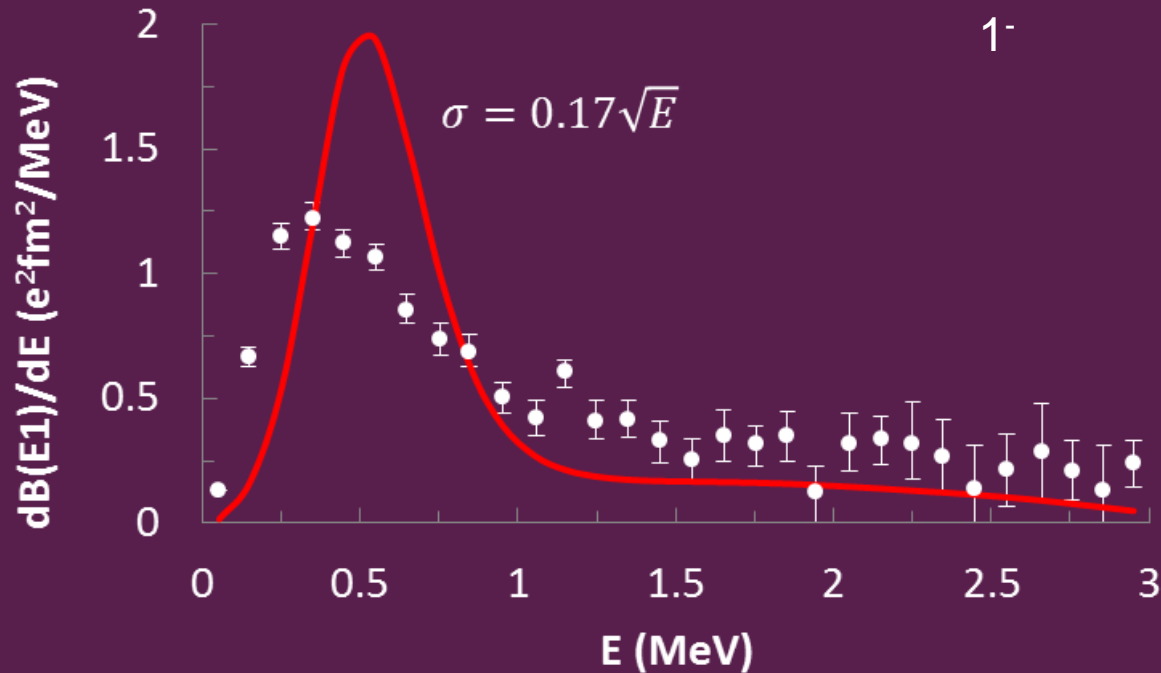


Fig 5. The  $\sigma$  value is in MeV. Experimental Data from *T. Nakamura et. al, Phys. Rev. Lett. 252502 (2006)*.

❖ We overestimate the E1 distribution in the peak region.

# Four-body breakup eikonal

- ⊙ Some applications by *D. Baye, P. Capel, P. Descouvemont and Y. Suzuki, Phys. Rev. C 71, 024607 (2009)*. They described the elastic breakup cross section of  ${}^6\text{He}$  on  ${}^{208}\text{Pb}$  @ 70 A MeV.
- ⊙ **Qualities of the model:**
  - ✓ Contributions different from the dipole.
  - ✓ It does not require  ${}^6\text{He}$ - ${}^{208}\text{Pb}$  potential:  $\alpha$ - ${}^{208}\text{Pb}$  potential and  $n$ - ${}^{208}\text{Pb}$  potential are well known.
  - ✓ It takes nuclear and Coulomb effects and their interference on the same footing.
  - ✓ There is not adjustable parameter.

# Conditions of the calculations for $^{11}\text{Li}$ on $^{208}\text{Pb}$

To calculate the breakup cross sections of  $^{11}\text{Li}$  on  $^{208}\text{Pb}$  @ 70 A MeV:

## ❖ $^9\text{Li}$ - $^{208}\text{Pb}$ potential (lack of the potential):

Renormalized  $(9^{1/3}+208^{1/3}) \alpha$ - $^{208}\text{Pb}$  interaction @ 70 A MeV of B. Bonin et. al. (Following the same idea of *P. Capel et. al, Phys. Rev. 68, 014612 (2003)* for  $^{10}\text{Be}$  on  $^{208}\text{Pb}$ ).

❖ Variation of the  $^9\text{Li}$ - $^{208}\text{Pb}$  potential was checked but it did not provide a significant change to the breakup and angular distributions.

## ❖ $n$ - $^{208}\text{Pb}$ potential:

Kooning and Delaroche, Nucl. Phys. A 713, 231 (2003).

# Breakup cross sections of $^{11}\text{Li}$ on $^{208}\text{Pb}$ @ 70 A MeV

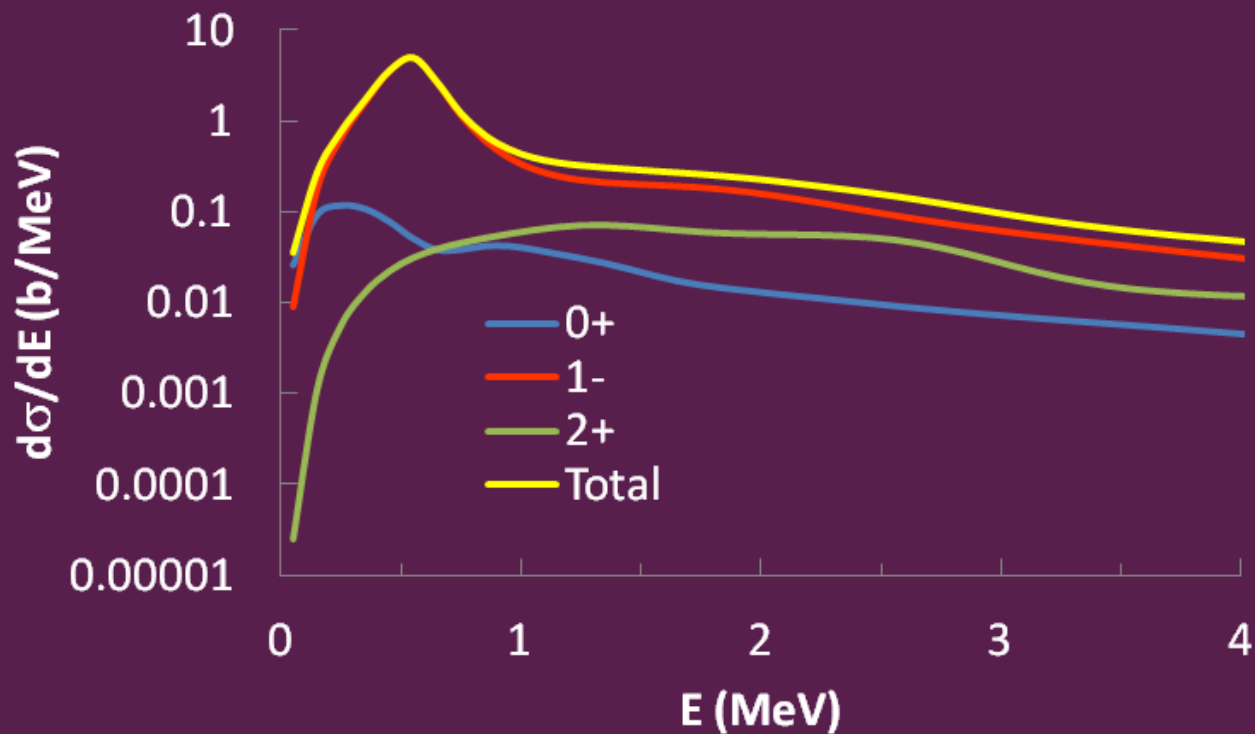


Fig. 6. Partial and total eikonal breakup cross sections.

❖ Small correction of the  $0+$  and  $2+$  partial waves to the total cross section.

# Convolutated breakup eikonal cross section with the detector response

$^{11}\text{Li}$  on  $^{208}\text{Pb}$  @ 70 A MeV

Theoretical data convoluted with a Gaussian of  $\sigma = 0.17\sqrt{E}$  MeV

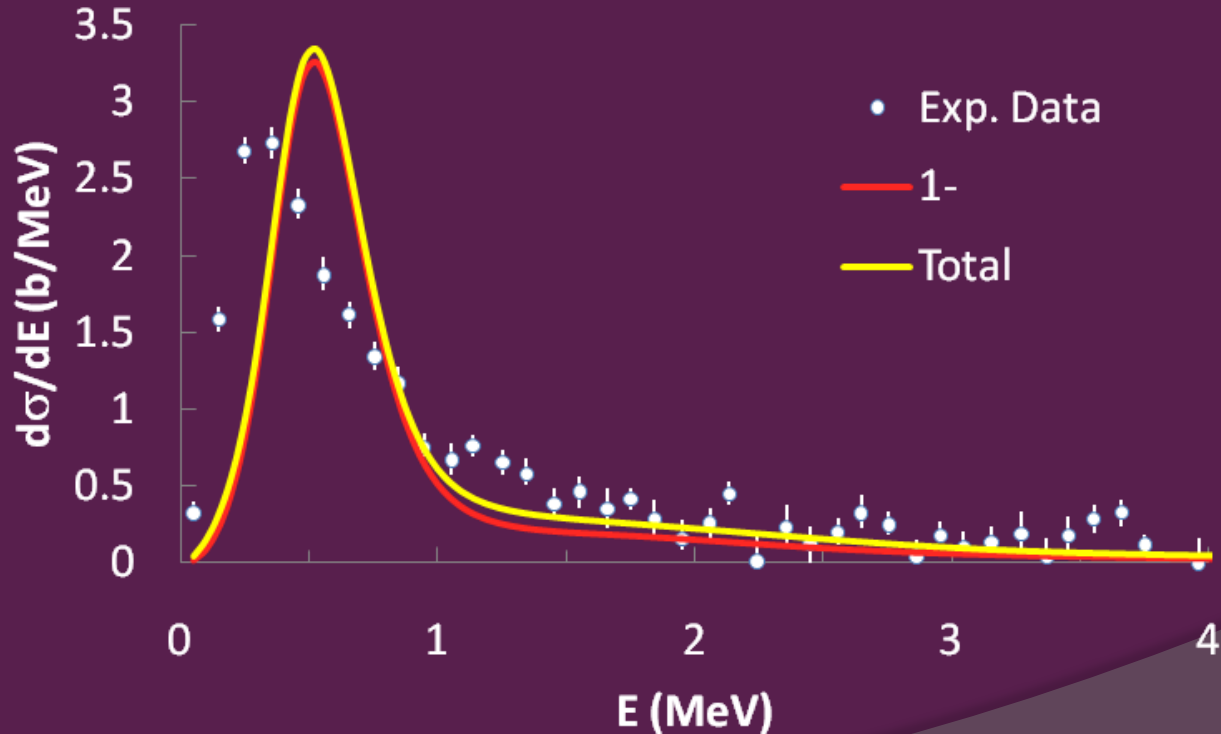


Fig. 7. Exp. Data from *T. Nakamura et. al, phys. Rev. Lett. 252502 (2006)*.



# Angular distributions of $^{11}\text{Li}$ on $^{208}\text{Pb}$ @ 70 A MeV

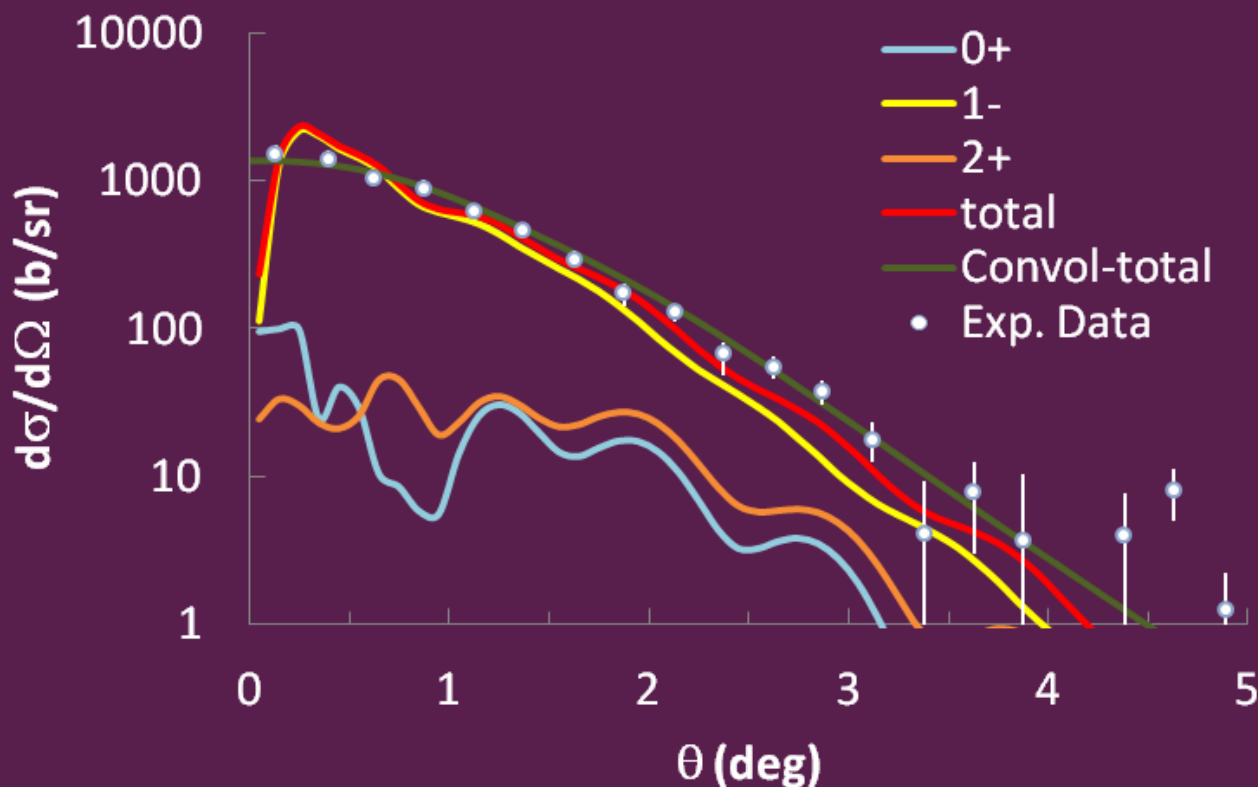


Fig. 8. Partial, total and convoluted total angular distributions. Experimental Data from *T. Nakamura et. al, Phys. Rev. Lett. 252502 (2006)*.

- ❖ Very good agreement of the total convoluted curve for almost all angles.
- ❖ Appreciable  $0^+$  and  $2^+$  contributions after  $\theta \gtrsim 1$  deg.

# Convoluting E1 strength distribution of $^{11}\text{Li}$ with the detector response

R-matrix (Red curve)

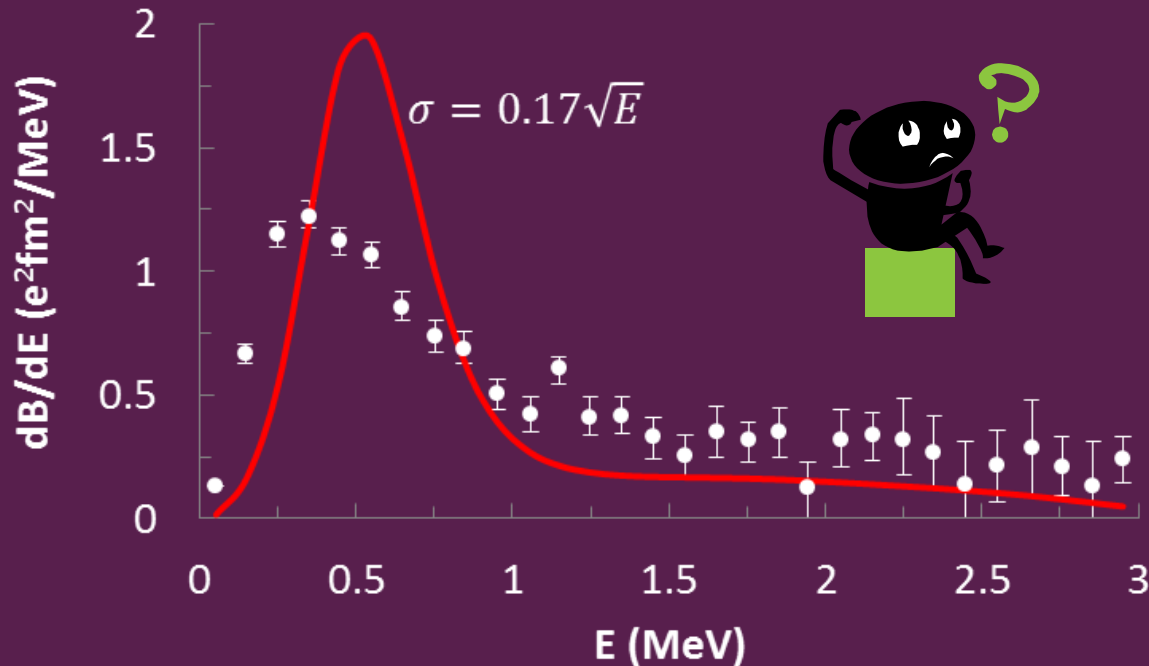


Fig. 9. The  $\sigma$  value is in MeV. Experimental Data from *T. Nakamura et. al, Phys. Rev. Lett. 252502 (2006)*.

❖ Why we overestimate the E1 distribution?

# Why we overestimate the E1 distribution?

In the breakup reactions of  $^{11}\text{Li}+^{208}\text{Pb}$  @ 70 A MeV

- ❖  $\frac{d\sigma}{dE}$  is measured directly  $\longrightarrow$  We fit the data
- ❖  $\frac{d\sigma}{d\theta}$  is measured directly  $\longrightarrow$  We fit the data
- ❖  $\frac{dB(E1)}{dE}$  is measured indirectly  
(It depends on model assumptions)  $\longrightarrow$  We do not fit the data

# How is determined experimentally $dB(E1)/dE$ ?

It is extracted from the equivalent photon method as

$$\frac{d\sigma^{\text{Exp}}}{dE} = \frac{16\pi^3}{9\hbar c} \frac{dB^{\text{Exp}}(E1)}{dE} \int_{b_{\min}}^{\infty} 2\pi db b N_{E1}(b, E)$$

- ❖ From  $b_{\min}$  to exclude nuclear excitation.
- ❖  $N_{E1}(b, E) \rightarrow$  Number of virtual photons incident on  $^{11}\text{Li}$  by unit area.
- ❖ It is assumed to be one step and dominated by a single E1 multipolar transition.
- ❖ It comes from semi-classical perturbation theory.



$^{11}\text{Li}$  is excited by absorption of a virtual photon from the Coulomb field of the target.

# Estimation of the $\theta_c$ dependence in the dipole distribution of $^{11}\text{Li}$

In non-relativistic regime

$$\frac{dB^{\text{Exp}}(E1)}{dE} = \frac{9}{32\pi} \left( \frac{\hbar v}{Z_T e} \right)^2 \frac{1}{\xi_{\min} K_0(\xi_{\min}) K_1(\xi_{\min})} \frac{d\sigma^{\text{Exp}}}{d\Omega}$$

$v \rightarrow$  Projectile-target relative velocity,

$$\xi_{\min} = \frac{E - E_0}{\hbar v} b_{\min},$$

$E \rightarrow$  Excitation energy of  $^{11}\text{Li}$ ,

$E_0 \rightarrow$  G. S. energy of  $^{11}\text{Li}$

$$b_{\min} = \frac{Z_P Z_T e^2}{2 \tan\left(\frac{\theta_c}{2}\right)} \rightarrow$$

Min. Impact parameter for the semi-classical Coulomb trajectory

$\theta_c \rightarrow$  maximum scattering angle (beyond  $\theta_c$  nuclear interaction is important.)

# Estimation of the $\theta_c$ dependence in the dipole distribution of $^{11}\text{Li}$

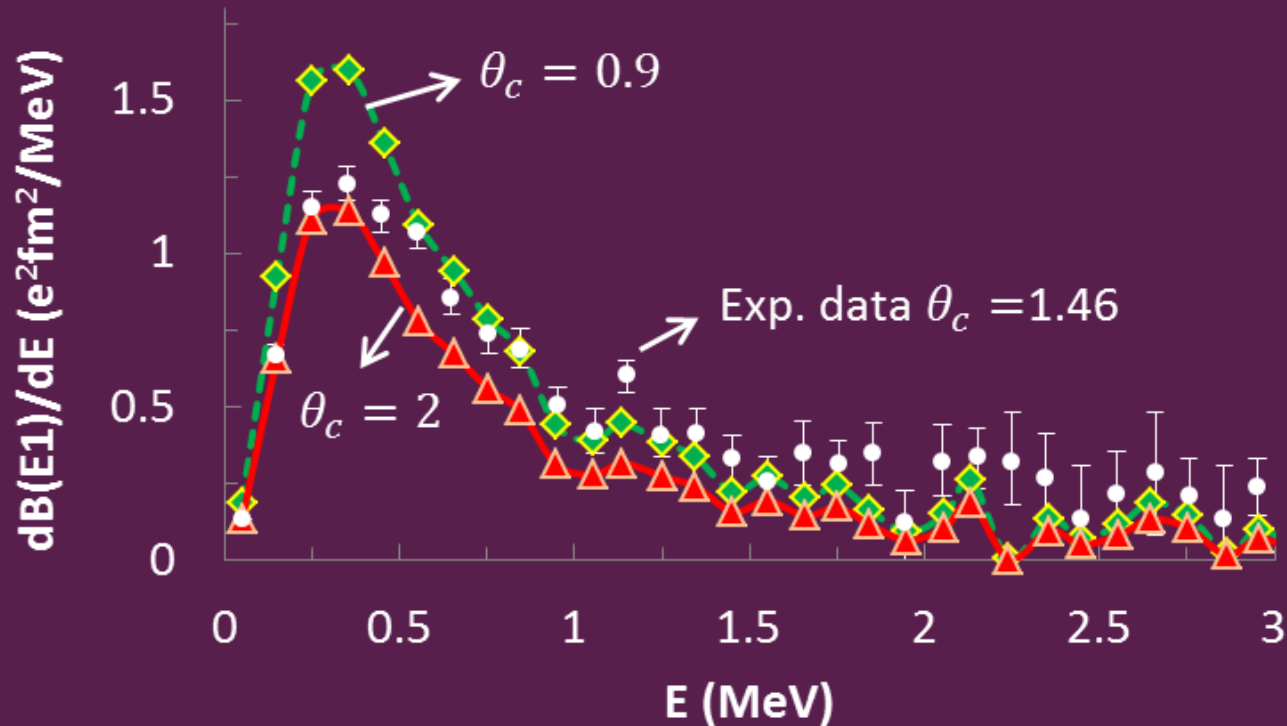


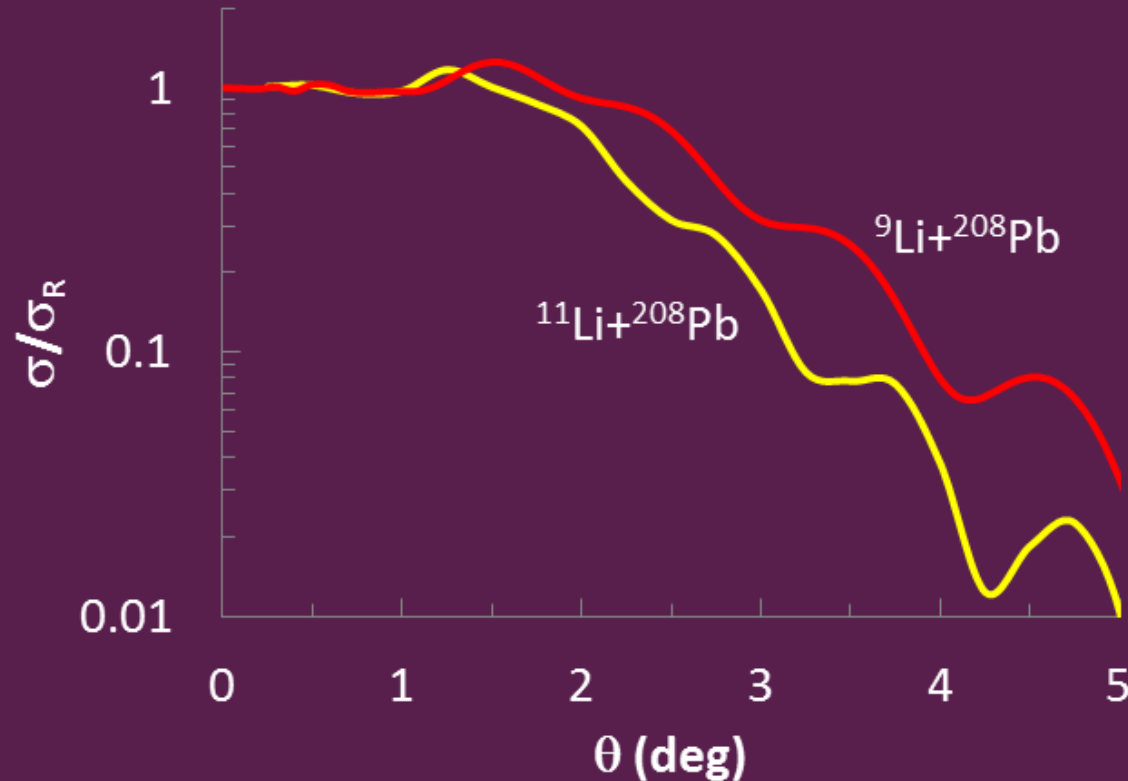
Fig. 10. The  $\theta_c$  values of 0.9, 1.46 and 2 deg correspond to  $b_{min}$  of 31, 19 and 14 fm respectively.

- ❖ Small  $\theta_c$  provides a larger dipole distribution at low excitation energies.

# Elastic scattering of $^{11}\text{Li}$ on $^{208}\text{Pb}$ @ 70 A MeV in the Eikonal method

Three-body projectile (yellow curve)

One-body projectile (red curve)



- ❖ Reduction in the  $^{11}\text{Li}+^{208}\text{Pb}$  elastic scattering due to flux going to breakup.
- ❖  $0 \lesssim \theta \lesssim 1 \rightarrow$  Rutherford scattering.

# Conclusions

- ❖ We have predicted a  $1^-$  resonant eigenphase for  $^{11}\text{Li}$ .
- ❖ The maximal contribution for the total breakup cross section is coming from the  $1^-$  partial wave.
- ❖ The breakup cross sections and angular distributions of  $^{11}\text{Li}$  on  $^{208}\text{Pb}$  are in good agreement with the experimental data.
- ❖ To test our model we suggest to experimentalist to measure elastic scattering of  $^{11}\text{Li}$  at high-energies.
- ❖ We need to clarify why we overestimate the dipole strength distribution of  $^{11}\text{Li}$  with the same  $^{11}\text{Li}$  wave functions that we had successful results for the breakup and angular distributions. Ideas are welcome!

Thank you for your attention